UNIVERSITÄT AUGSBURG
Universitätsbibliothek

OPEN ACCESS
OPUS AUGSBURG

Impact of tumor burden on quantitative [68Ga] DOTATOC biodistribution

Rudolf A. Werner, Heribert Hänscheid, Jeffrey P. Leal, Mehrbod S. Javadi, Takahiro Higuchi, Martin A. Lodge, Andreas K. Buck, Martin G. Pomper, Constantin Lapa, Steven P. Rowe

Angaben zur Veröffentlichung / Publication details:

Werner, Rudolf A., Heribert Hänscheid, Jeffrey P. Leal, Mehrbod S. Javadi, Takahiro Higuchi, Martin A. Lodge, Andreas K. Buck, Martin G. Pomper, Constantin Lapa, and Steven P. Rowe. 2018. "Impact of tumor burden on quantitative [68Ga] DOTATOC biodistribution." *Molecular Imaging and Biology* 21 (4): 790–98. https://doi.org/10.1007/s11307-018-1293-9.

Nutzungsbedingungen / Terms of use: **CC BY 4.0**

Dieses Dokument wird unter folgenden Bedingungen zur Verfügung gestellt: / This document is made available under these conditions:
CC-BY 4.0: Creative Commons: Namensnennung
Weitere Informationen finden Sie unter: / For more information see:
https://creativecommons.org/licenses/by/4.0/deed.de

MOLECULAR IMAGING AND BIOLOGY

Mol Imaging Biol (2019) 21:790–798
DOI: 10.1007/s11307-018-1293-9
© The Author(s), 2018
Published Online: 7 November 2018

RESEARCH ARTICLE

Impact of Tumor Burden on Quantitative [^{68}Ga] DOTATOC Biodistribution

Rudolf A. Werner,[1,2,3] Heribert Hänscheid,[1] Jeffrey P. Leal,[3] Mehrbod S. Javadi,[3] Takahiro Higuchi,[1] Martin A. Lodge,[3] Andreas K. Buck,[1,2] Martin G. Pomper,[3,4] Constantin Lapa,[1] Steven P. Rowe[3,4]

[1]*Department of Nuclear Medicine, University Hospital Wuerzburg, Wuerzburg, Germany*
[2]*European Neuroendocrine Tumor Society (ENETS) Center of Excellence, University Hospital Wuerzburg, Wuerzburg, Germany*
[3]*The Russell H. Morgan Department of Radiology and Radiological Science, Division of Nuclear Medicine and Molecular Imaging, Johns Hopkins University School of Medicine, 601 N. Caroline St, Baltimore, MD, 21287, USA*
[4]*James Buchanan Brady Urological Institute and Department of Urology, Johns Hopkins University School of Medicine, Baltimore, MD, USA*

Abstract

Purpose: As has been previously reported, the somatostatin receptor (SSTR) imaging agent [^{68}Ga]-labeled 1,4,7,10-tetraazacyclododecane-N,N′,N″,N‴-tetraacetic acid-d-Phe(1)-Tyr(3)-octreotate ([^{68}Ga]DOTATATE) demonstrates lower uptake in normal organs in patients with a high neuroendocrine tumor (NET) burden. Given the higher SSTR affinity of [^{68}Ga] DOTATATE, we aimed to quantitatively investigate the biodistribution of [^{68}Ga]-labeled 1,4,7,10-tetraazacyclododecane-N,N′,N″,N‴-tetraacetic acid-d-Phe(1)-Tyr(3)-octreotide ([^{68}Ga]DOTATOC) to determine a potential correlation between uptake in normal organs and NET burden.

Procedures: Of the 44 included patients, 36/44 (82 %) patients demonstrated suspicious radiotracer uptake on [^{68}Ga] DOTATOC positron emission tomography (PET)/X-ray computed tomography (CT). Volumes of interest (VOIs) were defined for tumor lesions and normal organs (spleen, liver, kidneys, adrenals). Mean body weight corrected standardized uptake value (SUV_{mean}) for normal organs was assessed and was used to calculate the corresponding mean specific activity uptake (Upt: fraction of injected activity per kg of tissue). For the entire tumor burden, SUV_{mean}, maximum standardized uptake value (SUV_{max}), and the total mass (TBM) was calculated and the decay corrected tumor fractional uptake (TBU) was assessed. A Spearman's rank correlation coefficient was used to determine the correlations between normal organ uptake and tumor burden.

Results: The median SUV_{mean} was 18.7 for the spleen (kidneys, 9.2; adrenals, 6.8; liver, 5.6). For tumor burden, the median values were SUV_{mean} 6.9, SUV_{max} 35.5, TBM 42.6 g, and TBU 1.2 %. With increasing volume of distribution, represented by lean body mass and body surface area (BSA), Upt decreased in kidneys, liver, and adrenal glands and SUV_{mean} increased in the spleen. Correlation improved only for both kidneys and adrenals when the influence of the tumor uptake on the activity available for organ uptake was taken into account by the factor 1/(1-TBU). TBU was neither predictive for SUV_{mean} nor for Upt in any of the organs. The distribution of organ Upt *vs.* BSA/(1-TBU) were not different for patients with minor TBU (<3 %) *vs.* higher TBU

Rudolf A. Werner, Heribert Hänscheid, Constantin Lapa and Steven P. Rowe contributed equally to this work.

Correspondence to: Steven Rowe; *e-mail:* srowe8@jhmi.edu

(>7 %), indicating that the correlations observed in the present study are explainable by the body size effect. High tumor mass and uptake mitigated against G1 NET.
Conclusions: There is no significant impact on normal organ biodistribution with increasing tumor burden on [^{68}Ga] DOTATOC PET/CT. Potential implications include increased normal organ dose with [^{177}Lu-DOTA]^{0}-D-Phe^{1}-Tyr^{3}-Octreotide and decreased absolute lesion detection with [^{68}Ga] DOTATOC in high NET burden.

Key words: Quantification, [^{68}Ga]DOTATOC, Neuroendocrine tumor, SSTR-PET, Theranostics, Somatostatin receptor

Introduction

Due to the recently published results of the NETTER-1 trial [1], Peptide Receptor Radionuclide Therapy (PRRT) is now US Food and Drug Administration approved and is becoming a clinical standard for the treatment of metastatic somatostatin receptor (SSTR)-expressing tumors [2, 3]. Sufficient uptake in neuroendocrine tumor (NET) lesions must be present on a pretherapeutic SSTR positron emission tomography (PET) scan using dedicated PET imaging agents, such as Ga-68 labeled 1,4,7,10-tetraazacyclododecane-N,N′,N″,N‴-tetraacetic acid-d-Phe(1)-Tyr(3)-octreotide/−octreotate ([^{68}Ga]DOTATOC/−TATE) or [^{68}Ga]DOTA,1-Nal3-octreotide ([^{68}Ga]DOTANOC) [4] in order for patients to potentially benefit from PRRT. Additionally, increasing interest in quantification of SSTR-targeted PET has come from recognition that quantitative uptake parameters might hold the potential to differentiate between responders and non-responders undergoing PRRT [5]. However, the biodistribution of a metabolic or receptor-targeting radiopharmaceutical agent is not in a "steady state," but is instead prone to a continuous complex interplay of uptake, retention, and excretion in both tumor lesions and non-affected organs with relevant SSTR expression on the cell surface [6]. Consequently, further insights into quantitative uptake parameters on SSTR-targeted PET among patients with different tumor burdens are needed.

One aspect of the interpretation of tumor molecular imaging is the influence of tumor uptake on the normal organ biodistribution. High tumor uptake can lead to a significant decrease in radiotracer uptake in other organs such as the kidneys [7, 8]. Beauregard et al. studied this phenomenon using the SSTR imaging agent [^{68}Ga] DOTATATE in a cohort of ten patients with varying tumor burden. They reported that higher tumor burden correlated with lower uptake in normal organs and suggested adapting the therapeutic activity to the tumor load [9].

In the present study, we quantitatively investigated the biodistribution of [^{68}Ga] DOTATOC to determine if a correlation between uptake in normal organs and tumor burden exists and if tumor uptake in PET could theoretically be used to modify the therapeutic administered activity of [^{177}Lu-DOTA]^{0}-D-Phe^{1}-Tyr^{3}-Octreotide ([^{177}Lu]DOTATOC). Such a correlation might also have implications for diagnostic image interpretation. Apart from that, we aimed to elucidate if a relationship between histological derived tumor grade and the activity distribution exists and if the tumor stage can be reproduced from the information deduced from PET imaging.

Materials and Methods

Medical reports of 44 consecutive patients with histopathologically proven NET grade 1 or 2 who underwent [^{68}Ga] DOTATOC PET/X-ray computed tomography (CT) imaging were reviewed in this retrospective evaluation. Of these patients, 36/44 (82 %) had clinical PET/CT reads indicating the presence of suspicious, non-physiological radiotracer uptake compatible with sites of NET. At the time of imaging, all patients had signed written informed consent to the medical examination and to the retrospective use of the anonymized data. Requirement for additional approval for this analysis was waived due to the retrospective character of this study.

Imaging Procedure

All patients underwent [^{68}Ga] DOTATOC PET/ CT, with application of contrast media in 42/44 (95.5 %) according to current guidelines for the assessment of SSTR expression [10]. Integrated PET/CT using a Siemens Biograph 64 (Siemens Medical Solution, Erlangen, Germany) operating in 3D emission mode with CT attenuation correction was performed in all patients. [^{68}Ga] DOTATOC (median, 125 MBq, 3.4 mCi) was injected intravenously and after 60 min, acquisitions from the mid-thigh to the vertex of the skull were conducted, covering six to eight bed positions (depending on patient height) with patients in the supine position. All data was reconstructed using iterative algorithms implemented by the manufacturer. For further details, please refer to [11].

Image Analysis

PET images were analyzed using XD3 Software (Mirada Medical, Oxford, UK). PET, CT, and hybrid PET/CT imaging overlay were assessed in all 44 patients. Lesions

Table 1.. Patient's characteristics according to grading

Case	Sex	Age (years)	GEP-NET (Y = yes, N = no)	VOI localization on baseline SSTR-targeted PET	Prior therapy	Grading
#1	f	62	Y	n/a	Surgery	1
#2	m	52	Y	n/a	Surgery	1
#3	m	55	Y	n/a	Surgery	1
#4	m	31	Y	n/a	Surgery	1
#5	m	56	Y	n/a	None	1
#6	m	60	Y	n/a	Surgery	1
#7	f	79	Y	n/a	None	1
#8	f	72	N (CUP)	LN, bone, liver, soft tissue	Surgery, SSA, CTx, TKI	1
#9	m	76	N (CUP)	LN, liver, bone	SSA	1
#10	f	51	Y	LN, bone, liver	Surgery, SSA, PRRT	1
#11	f	73	Y	LN	SSA	1
#12	m	47	N (lung NET)	Lung	None	1
#13	f	77	Y	Soft tissue	Surgery, SSA, CTx	1
#14	m	83	Y	Soft tissue	SSA	1
#15	f	44	Y	Bone	None	1
#16	m	75	N (CUP)	LN, soft tissue	Surgery, SSA	1
#17	f	77	Y	LN, bone, liver, soft tissue	SSA, PRRT, CTx	1
#18	m	65	Y	LN, liver, soft tissue	Surgery, SSA, PRRT, CTx	1
#19	f	61	Y	Liver	Surgery, SSA	1
#20	f	58	Y	Bone, liver, soft tissue	Surgery, SSA, PRRT	1
#21	m	53	Y	LN, bone, soft tissue	PRRT	1
#22	m	67	N (CUP)	Soft tissue	Surgery, CTx	2
#23	f	50	N (lung NET)	Soft tissue	None	2
#24	m	74	Y	Liver	Surgery	2
#25	m	67	Y	LN, bone	Surgery, SSA, PRRT, LP	2
#26	f	42	Y	LN, liver	Surgery	2
#27	m	57	Y	Liver, soft tissue	SSA, PRRT	2
#28	f	69	Y	LN, bone, lung	SSA, PRRT, LP	2
#29	m	64	Y	Liver	PRRT	2
#30	f	68	Y	LN	Surgery	2
#31	m	70	Y	LN, liver, soft tissue	SSA, PRRT, CTx	2
#32	f	72	Y	Liver, soft tissue	Surgery, SSA, PRRT, CTx	2
#33	f	74	Y	Liver, soft tissue	Surgery, SSA	2
#34	m	66	Y	Liver, soft tissue	None	2
#35	m	52	Y	LN, liver, soft tissue	SSA, PRRT	2
#36	f	63	Y	Soft tissue	Surgery	2
#37	m	65	Y	LN, bone, liver, soft tissue	Surgery, SSA, PRRT	2
#38	m	57	Y	LN, liver, soft tissue	Surgery, SSA	2
#39	f	51	Y	Liver, soft tissue	Surgery	2
#40	f	49	Y	LN, liver	SSA, PRRT	2
#41	m	77	Y	LN, soft tissue	Surgery	2
#42	f	61	Y	n/a	Surgery	2
#43	f	53	Y	Bone	Surgery, SSA, PRRT, CTx, LP	2
#44	m	72	Y	Liver	Surgery	2

CTx chemotherapy, CUP cancer of unknown primary, f female, GEP-NET gastroenteropancreatic neuroendocrine tumor, LN lymph node, m male, LP locoregional procedure, PRRT peptide receptor radionuclide therapy, RTx radiation therapy, SSA somatostatin analog, SSTR-targeted PET somatostatin receptor-targeted positron emission tomography

were identified as abnormal foci of radiotracer uptake above background and in expected patterns based on the patients' original tumor histologies. Lesions were selected by a single reader and verified by a second reader.

With the normal biodistribution of [^{68}Ga] DOTATOC, at least moderate uptake is typically observed in spleen, liver, both kidneys, and both adrenal glands [12]. For these organs, volumes of interest (VOIs) were manually drawn covering the entire organ volume using the best visual approximation of the organ edge on the PET images as has previously been described [13, 14]. In addition, the entire volume of all [^{68}Ga]DOTATOC-avid tumor lesions (*i.e.*, tumor burden) was manually segmented using the same procedure. As shown in [14], the CT images were not used to guide delineation of the VOIs, except in the case of patients with liver metastases in which liver lesions and normal liver tissue were carefully separated using PET, CT, and hybrid PET/CT, as necessary.

The following parameters were assessed for the normal organs: the mean body weight corrected standardized uptake value (SUV_{mean}) was measured for the spleen and the liver as well as for both kidneys and both adrenal glands for which the final values were derived as mean values of the right and left organs. The SUV_{mean} were used to calculate the corresponding mean specific activity uptake (Upt: fraction of injected activity per kg of tissue).

For the entire tumor burden, SUV_{mean} and maximum standardized uptake value (SUV_{max}) as well as the total mass (TBM) and the decay corrected tumor fractional uptake (TBU) were determined. TBU was calculated as sum of the

Table 2.. Descriptive statistics of normal organs and tumor burden

Compartment	Parameter	Patients	Minimum	Median	Maximum	Mean*	StDev*
Spleen	SUV_{mean}	42	3.6	18.7	36.9	18.7	7.3
Kidneys	SUV_{mean}	44	3.2	9.2	19.7		
Adrenal glands	SUV_{mean}	43	0.5	6.8	13.3	6.7	2.3
Liver	SUV_{mean}	44	2.4	5.6	14.6		
Tumor burden	SUV_{mean}	35	1.6	6.9	36.7		
	SUV_{max}	35	4.3	35.5	109.4		
	TBM	36	2.2 g	42.6 g	3190 g		
	TBU	36	0.01 %	1.2 %	27.7 %		

Maximum/mean standardized uptake value ($SUV_{max/mean}$), total tumor mass (TBM), and the decay-corrected tumor fractional uptake (TBU). Asterisk indicates that mean and standard deviation (StDev) are not shown when the Shapiro-Wilk test excluded a normal distribution. Two spleens could not be assessed due to splenectomy. In one patient, both adrenal glands were unidentifiable. One patient with only two small lesions <15 mm was excluded from SUV statistics

products [lesion mass / body mass × SUV_{mean}] of all evaluated tumor lesions assuming density 1 g/cm^3 for tumor lesions. Metastases smaller than 15 mm (< 1.7 cm^3) were not included in the calculation of SUV statistics to avoid partial volume effects (PVE).

The volume of distribution influences the mean activity concentration in the body and thus potentially activity uptake in organs and tumors. Following the procedure in [9], James' lean body mass estimate (LBM) and Mosteller's body surface estimate area (BSA) were used as surrogate parameters for the volume of distribution [15, 16].

Moreover, to investigate whether tumor grading (G1 *vs.* G2) can be confirmed non-invasively by PET, a potential relationship between tumor grading and the activity distribution was examined.

Table 3.. Correlation between parameters

Parameter		Kidneys		Spleen		Liver		Adrenals	
		SUV_{mean}	Upt	SUV_{mean}	Upt	SUV_{mean}	Upt	SUV_{mean}	Upt
Kidneys SUV_{mean}	ρ			.48		0.17		0.13	
	P			**0.001**		0.27		0.41	
	N			42		44		43	
Upt	ρ				0.38		0.26		0.48
	P				**0.01**		0.08		**0.001**
	N				42		44		43
Spleen SUV_{mean}	ρ					0.61		0.21	
	P					**2E−5**		0.19	
	N					42		41	
Upt	ρ						0.67		0.25
	P						**1E−6**		0.11
	N						42		41
Liver SUV_{mean}	ρ							0.18	
	P							0.26	
	N							43	
Upt	ρ								0.23
	P								0.14
	N								43
TBU	ρ	− 0.29	− 0.09	− 0.40	− 0.14	0.09	0.27	− 0.32	− 0.09
	P	0.06	0.58	**0.008**	0.39	0.56	0.08	**0.04**	0.59
	N	44	44	42	42	44	44	43	43
LBM	ρ	0.19	− 0.45	0.37	− 0.15	0.18	− 0.34	0.23	− 0.35
	P	0.22	**0.002**	**0.02**	0.34	0.24	**0.03**	0.14	**0.02**
	N	44	44	42	42	44	44	43	43
LBM 1-TBU	ρ	0.11	− 0.52	0.29	− 0.19	0.22	− 0.27	0.12	− 0.41
	P	0.49	**3E−4**	0.06	0.23	0.16	0.07	0.46	**0.007**
	N	44	44	42	42	44	44	43	43
BSA	ρ	0.22	− 0.44	0.34	− 0.23	0.13	− 0.43	0.24	− 0.39
	P	0.14	**0.003**	**0.03**	0.14	0.42	**0.004**	0.12	**0.009**
	N	44	44	42	42	44	44	43	43
BSA 1-TBU	ρ	0.06	− 0.57	0.21	− 0.28	0.19	− 0.32	0.03	− 0.49
	P	0.69	**5E−5**	0.19	0.07	0.22	**0.03**	0.85	**8E−4**
	N	44	44	42	42	44	44	43	43

Spearman's rho (ρ), the two-sided significance P (bold for significant correlations), and the number N of patients included are shown
SUV_{mean} mean standardized uptake value, Upt fractional uptake per volume of tissue, TBU total fractional tumor uptake, LBM lean body mass estimate, BSA body surface estimate

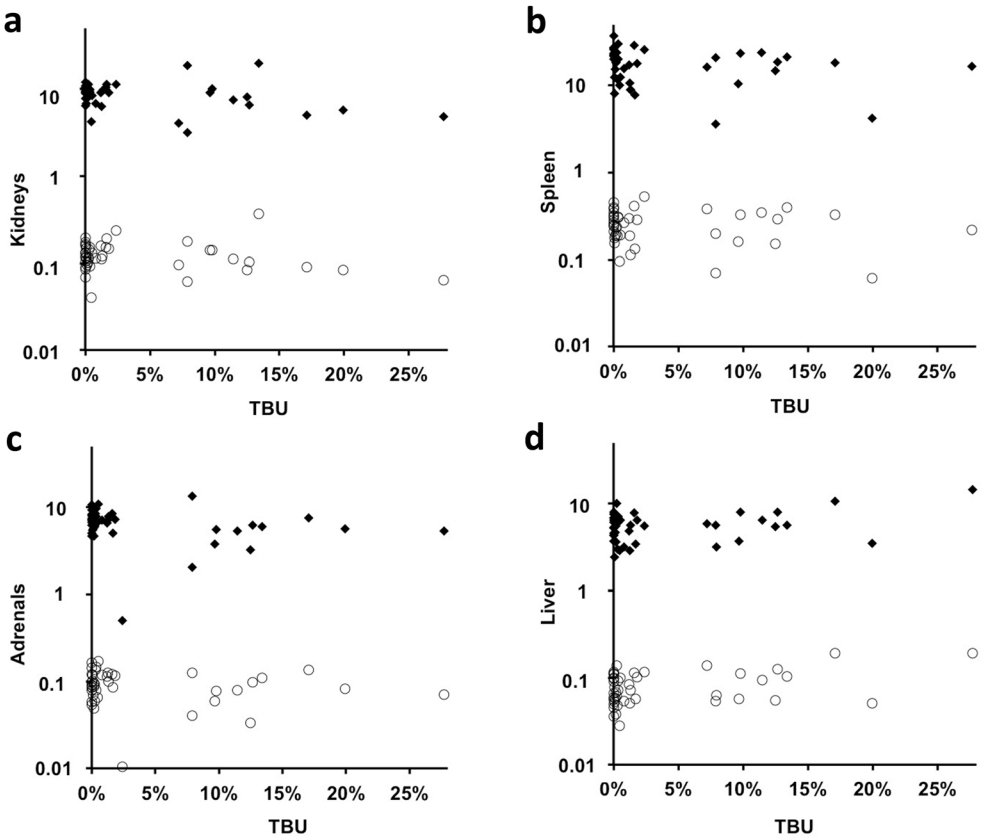

Fig. 1 Mean standardized uptake value (SUV_{mean}; rhombs) and fraction of injected activity per kilogram of tissue (Upt; circles) in normal organs (**a** kidneys, **b** spleen, **c** adrenals, and **d** liver) *vs.* decay corrected tumor fractional uptake (TBU).

Statistical Analysis

Statistical analysis was performed using SPSS Statistics 25. Percentiles are reported to describe the distributions of the parameters. Additionally, mean ± standard deviation is displayed for parameters if a normal distribution is not excluded by the Shapiro-Wilk test. Spearman's rank correlation coefficient was used to assess the correlations between parameters. Mann-Whitney *U* test was used to investigate differences between tumor grading. A *p* value of less than 0.05 was assumed to be statistically significant.

Results

Patient Population

A total of 44 patients (21 females; median age 64 years; mean age 62.4 ± 11.5 years; range 31–79 years) who underwent [68Ga] DOTATOC were quantitatively analyzed. Out of 44 (86.4 %), 38 had a history of gastroenteropancreatic NET (primary: ileum/jejunum/mesentery, 24/38, 63.2 %; pancreas, 10/38, 26.3 %; colon, 1/38, 2.6 %; rectum, 3/38, 7.9 %). In the remaining 6/44 (13.6 %), a neuroendocrine tumor of the lung (2/6, 33.3 %) or a cancer of unknown primary (4/6, 66.7 %) had been diagnosed. The clinical indication for imaging was evaluation of recurrent/metastatic disease in the majority of patients (33/44, 75.0 %), while the remainder underwent [68Ga] DOTATOC PET/CT for staging (11/44, 25.0 %). The median Ki67 was 4 % (mean, 5.3 ± 4.5 %). Out of 44 (47.7 %), 21 were G1 NET, while the remaining 23/44 (52.3 %) were G2 NET. Out of 44 (86.4 %), 38 of the enrolled patients had undergone previous therapy (surgery, 27/38 (71.1 %); "cold" somatostatin analogues, 22/38 (57.9 %); PRRT, 15/38 (39.5 %); chemotherapy, 8/38 (21.1 %); prior locoregional therapy, 3/38 (7.9 %); and tyrosine kinase inhibitor therapy 1/38, (2.6 %)). The remaining 6/44 (13.6 %) were treatment-naive at the time of imaging. Table 1 summarizes these patients' parameters.

Quantitative Assessment

In one patient, both adrenal glands were unidentifiable. The right adrenal glands could not be identified in another two patients (in all cases as a result of an inability to visually separate the adrenal glands from adjacent organs on either the PET or CT portion of the examination). The right kidney could not be assessed in one patient due to a prior nephrectomy, and in one case, a horseshoe kidney was

evaluated as a right kidney (due to the fact that the main part of the organ was located in the right hemi-abdomen). Two spleens could not be assessed due to splenectomy.

To generate the data for tumor burden in the 36 patients demonstrating discernible, suspicious radiotracer uptake, a total of 182 VOIs were placed (median, 4 per patient; range, 1–23). Of these VOIs, 56/182 (30.8 %) included metastases in the skeleton, 53/182 (29.1 %) represented involved lymph nodes, 38/182 (20.9 %) corresponded to liver lesions, 33/182 (18.1 %) were non-nodal soft tissue lesions, and 2/182 (1.1 %) were lung nodules. One patient with only two small lesions <15 mm was excluded from SUV statistics.

Descriptive statistics are listed in Table 2. The median SUV_{mean} was 18.7 for the spleen, 9.2 for the kidneys, 6.8 for the adrenal glands, and 5.6 for the liver. For tumor burden, the median values were SUV_{mean}: 6.9, SUV_{max}: 35.5, TBM: 42.6 g, and TBU: 1.2 %.

Correlative Analysis Table 3 lists Spearman's rho for the relations between normal organ parameters, the tumor burden, and body size. The following significant relations were observed: when comparing the organs, both spleen SUV_{mean} and Upt correlated positively with the corresponding values in liver and kidneys. For the adrenals, only Upt correlated with kidney Upt. Negative correlation with TBU was observed for SUV_{mean} in spleen and adrenals.

With increasing volume of distribution, represented by LBM and BSA, Upt decreased in kidneys, liver, and adrenal glands and SUV_{mean} increased in the spleen. Correlation improved for the kidneys and the adrenals but not for liver and spleen when the influence of the tumor uptake on the activity available for organ uptake was taken into account by the factor 1/(1-TBU). Figure 1 shows the observed SUV_{mean} and Upt *vs.* TBU for the evaluated organs. Figure 2 shows the specific organ uptake Upt *vs.* BSA/(1-TBU); no difference is visible in the distributions for patients with minor (circles; TBU < 3 %) and higher tumor uptake (rhombs; TBU > 7 %).

In the groups of patients with tumor grade 1 and 2, there were no differences in the SUV values according to the Mann-Whitney *U* test. However, the total tumor mass tended to be higher ($P = 0.05$) and TBU was higher ($P = 0.03$) in patients with NET grade 2. Only one of eight patients with negative PET was grade 2.

Figure 3 displays three patients with different tumor burden (low, intermediate, high) and reflects visually that no significant decrease in normal organ uptake is appreciated with higher levels of tumor burden.

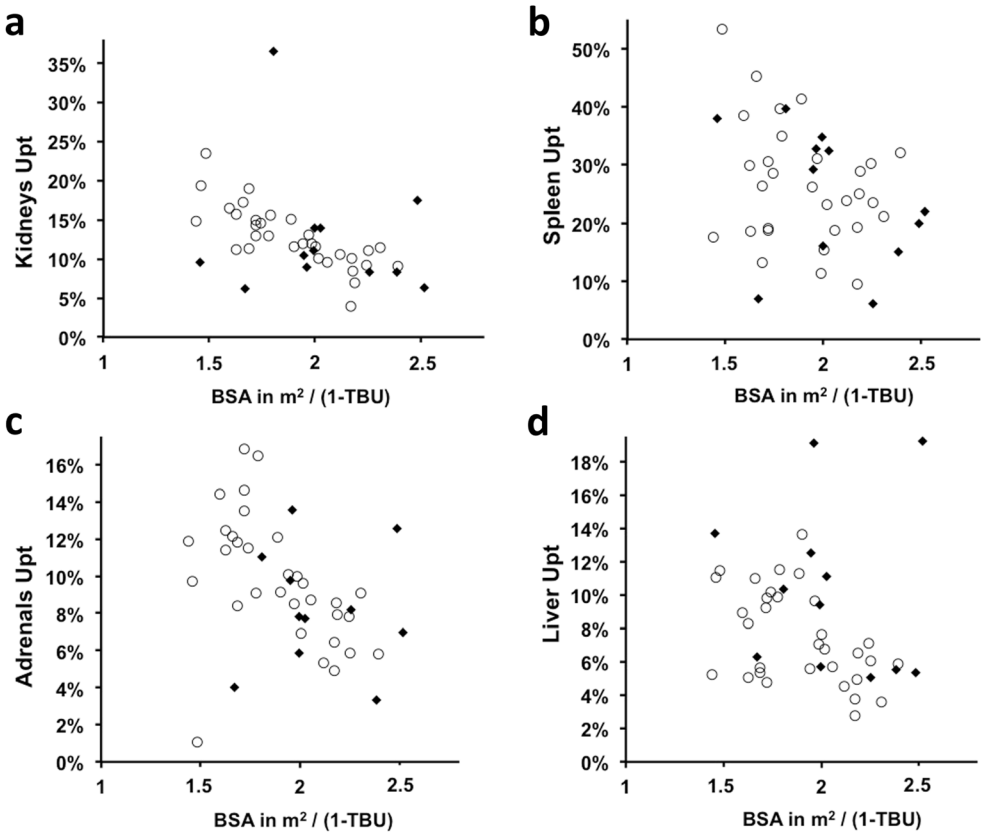

Fig. 2 Fraction of injected activity per kilogram of normal organ tissue (Upt) in **a** kidneys, **b** spleen, **c** adrenals, and **d** liver, in patients with total tumor uptake TBU < 3 % (circles) and TBU > 7 % (rhombs) as a function of the body surface area (BSA) modified by the factor 1/(1-TBU).

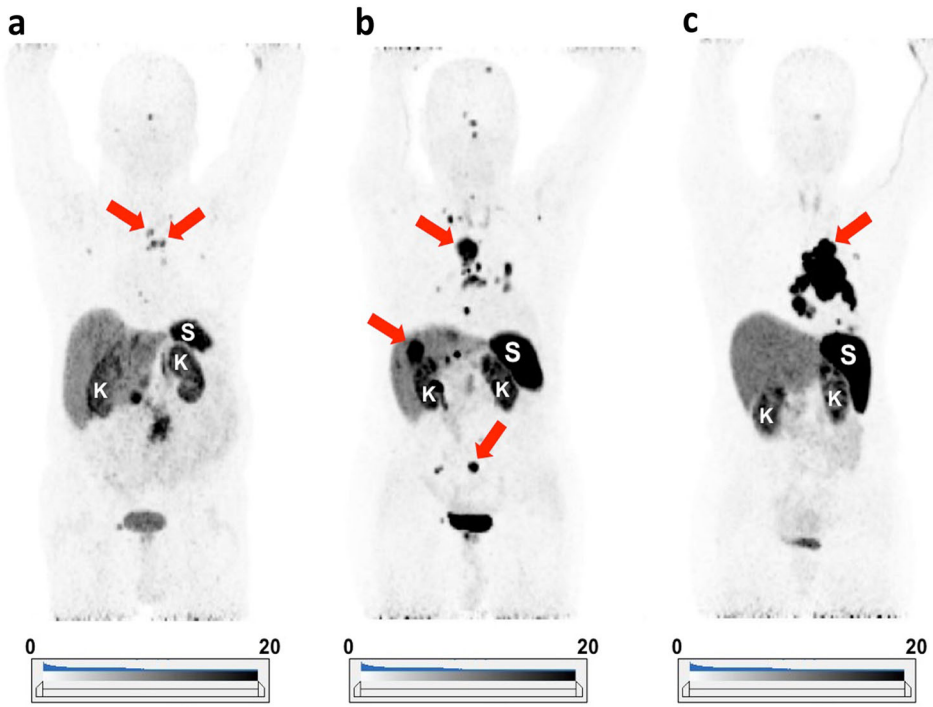

Fig. 3 The [^{68}Ga]DOTA-D-Phe-Tyr3-octreotide ([^{68}Ga]DOTATOC) maximum intensity projection (MIP) of patients with **a** low tumor burden, **b** intermediate tumor burden, and **c** high tumor burden. Spleen (S) and kidneys (K) are indicated. Threshold is set to a SUV of 20 (screenshots of XD3 software, Mirada medical, Oxford, UK, are displayed). Red arrows indicate tumor lesions, which can be detected on the MIP. **a** Several pulmonal lymph node metastases are indicated. **b** Lymph nodes, bone, and liver lesions are marked. **c** The primary in the lung is highlighted. The uptake in normal organs (visible for liver, kidneys, and spleen) does not differ among the different patients.

Discussion

In the present study in which the quantitative biodistribution of [^{68}Ga] DOTATOC was investigated in organs and tumors, we were unable to generate evidence to suggest that [^{177}Lu] DOTATOC endoradiotherapy doses should be modified on the basis of tumor burden. Although Spearman's rank test identified some correlation between tumor burden and normal abdominal organ uptake (Table 3), it can be seen in Fig. 1 that the total tumor uptake TBU is neither predictive for SUV_{mean} nor for the activity uptake Upt in any of the organs considered in this study.

Previously, the similar SSTR-targeted radiotracer [^{68}Ga] DOTATATE had demonstrated a tumor sink effect in a smaller ($n = 10$) and more homogeneous patient cohort [9]. [^{68}Ga] DOTATATE has a higher affinity for the SSTR2A receptor (IC_{50} 0.2 nM *vs.* 2.5 nM for [^{68}Ga]DOTATOC) [17] and median tumor uptake was higher in ref. [9] than in the present study, presumably giving rise to a larger dynamic range within a sink effect might be observed. Nevertheless, this effect was observed in our study as well. As in [9], all coefficients of correlation between the body size parameters and Upt were negative for all abdominal organs (Table 3). Correlations reached significance for kidneys, liver, and adrenal glands but not for the spleen. The generally observed positive correlation between SUV_{mean} and the body size parameters LBM and BSA was significant for the spleen only. However, compared to Beauregard at al. [9], it is possible that the tumor burden of the current patient cohort was relatively too low to observe a more robust tumor sink effect.

It can be seen in Fig. 2 that the distributions of organ Upt *vs.* BSA/(1-TBU) are not visibly different for patients with no or minor tumor uptake and those with TBU > 7 %, indicating that the correlations observed in the present study are completely explainable by the body size effect. Moreover, BSA/(1-TBU) cannot be used to predict the activity concentration in the kidneys (Fig. 2) and to modify the activity in a subsequent treatment accordingly, as it has been suggested in [9]. We agree that it can be helpful, particularly for patients with high tumor burden to adjust the therapy activity individually; however, the large variation in data would lead to high and unjustified corrections in many of the patients. Moreover, there is no validated method to determine the kidney dose from PRRT in advance from the activity concentration measured in PET. Considering the [^{68}Ga]/[^{177}Lu] DOTATOC theranostics pair, the physical half-life of Ga-68 is too short to predict biokinetics with Lu-177 with sufficient accuracy. Therefore, we recommend organ dosimetry with Lu-177 prior to the administration of unusually high therapeutic activities.

As there was no meaningful effect of tumor burden on normal organ uptake, this might also have implications for

the detection rate of tumor lesions, as the [68Ga] DOTATOC background uptake is not reduced in patients with high tumor burden (Fig. 3). This could potentially lead to readers missing lesions with subtle uptake near sites of significant tumor burden or normal organs with high expression levels of SSTR2. This would likely be a rare occurrence and would not affect staging in the vast majority of patients; however, a whole-body assessment with an SSTR-targeted PET imaging agent may benefit from the incorporation of structured reporting guidelines that include a measure of uncertainty when characterizing lesions [12].

In regard to our hypothesis that tumor grading may be suggested by PET findings, one of our intentions was to find a relationship between tumor grade and the activity distribution. Uptake in the abdominal organs turned out to be independent of grading. High tumor mass and uptake mitigated against, and a negative PET favored, grade 1. An attempt to reproduce tumor stage from the information deduced from PET imaging by a logistic binary regression resulted in a rate of correct prediction of less than 70 % (data not shown). It can therefore be concluded that PET is inadequate to identify or modify tumor grading non-invasively.

A limitation regarding the validity of the present study is that most of the patients in the cohort were heavily pretreated, which might have potentially biased the derived uptake values [18]. However, this enrolled cohort of randomly selected patients is reflective of a "real-world" clinical scenario in which patients being evaluated for PRRT will often have undergone prior treatments. Moreover, the herein obtained SUVs are generally similar to those reported from other studies using [68Ga]DOTA-based agents; compared to previous studies using [68Ga] DOTATOC, we derived almost identical values for normal organs (*e.g.*, for the spleen) [19, 20]. However, a dosimetry assessment with [177Lu] DOTATOC is definitely warranted to further explore whether a potential tumor sink effect exists with this radiotracer in a therapeutic setting. Apart from that, metastases smaller than 15 mm were excluded in the present investigation because of a potential PVE. However, a potential spill-in/spill-out phenomenon, possibly partially compensating for PVE, has been described for 2-deoxy-2-[18F]-fluoro-D-glucose and such an effect should be investigated for SSTR-targeted radiotracers as well [21].

Conclusion

In quantitative assessment of [68Ga] DOTATOC PET/CT, we found no significant effect of the tumor burden or the grading on normal organ uptake in a typical cohort of NET patients. [68Ga] DOTATOC PET/CT is inadequate to identify or modify tumor grading or serve as a substitute for dosimetry in order to justify administration of unusually high treatment activities.

Funding This project has received funding from the European Union's Horizon 2020 Research and Innovation Programme under the Marie Sklodowska-Curie grant agreement no. 701983.

Compliance with Ethical Standards

Conflict of Interest

The authors declare that they have no conflict of interest.

Open Access This article is distributed under the terms of the Creative Commons Attribution 4.0 International License (http://creativecommons.org/licenses/by/4.0/), which permits unrestricted use, distribution, and reproduction in any medium, provided you give appropriate credit to the original author(s) and the source, provide a link to the Creative Commons license, and indicate if changes were made.

References

1. Strosberg J, El-Haddad G, Wolin E et al (2017) Phase 3 trial of 177Lu-Dotatate for midgut neuroendocrine tumors. N Engl J Med 376:125–135
2. Bodei L, Ambrosini V, Herrmann K, Modlin I (2017) Current concepts in 68Ga-DOTATATE imaging of neuroendocrine neoplasms: interpretation, biodistribution, dosimetry, and molecular strategies. J Nucl Med 58:1718–1726
3. Werner RA, Bluemel C, Allen-Auerbach MS, Higuchi T, Herrmann K (2015) 68Gallium- and 90yttrium-/177lutetium: "theranostic twins" for diagnosis and treatment of NETs. Ann Nucl Med 29:1–7
4. Bodei L, Mueller-Brand J, Baum RP, Pavel ME, Hörsch D, O'Dorisio MS, O'Dorisio TM, Howe JR, Cremonesi M, Kwekkeboom DJ, Zaknun JJ (2013) The joint IAEA, EANM, and SNMMI practical guidance on peptide receptor radionuclide therapy (PRRNT) in neuroendocrine tumours. Eur J Nucl Med Mol Imaging 40:800–816
5. Kratochwil C, Stefanova M, Mavriopoulou E, Holland-Letz T, Dimitrakopoulou-Strauss A, Afshar-Oromieh A, Mier W, Haberkorn U, Giesel FL (2015) SUV of [68Ga]DOTATOC-PET/CT predicts response probability of PRRT in neuroendocrine tumors. Mol Imaging Biol 17:313–318
6. Prasad V, Baum RP (2010) Biodistribution of the Ga-68 labeled somatostatin analogue DOTA-NOC in patients with neuroendocrine tumors: characterization of uptake in normal organs and tumor lesions. Q J Nucl Med Mol Imaging 54:61–67
7. Liu Y (2011) Super-superscan on a bone scintigraphy. Clin Nucl Med 36:227–228
8. Manier SM, Van Nostrand D (1984) Super bone scan. Semin Nucl Med 14:46–47
9. Beauregard JM, Hofman MS, Kong G, Hicks RJ (2012) The tumour sink effect on the biodistribution of 68Ga-DOTA-octreotate: implications for peptide receptor radionuclide therapy. Eur J Nucl Med Mol Imaging 39:50–56
10. Virgolini I, Ambrosini V, Bomanji JB, Baum RP, Fanti S, Gabriel M, Papathanasiou ND, Pepe G, Oyen W, de Cristoforo C, Chiti A (2010) Procedure guidelines for PET/CT tumour imaging with 68Ga-DOTA-conjugated peptides: 68Ga-DOTA-TOC, 68Ga-DOTA-NOC, 68Ga-DOTA-TATE. Eur J Nucl Med Mol Imaging 37:2004–2010
11. Werner RA, Weich A, Higuchi T, Schmid JS, Schirbel A, Lassmann M, Wild V, Rudelius M, Kudlich T, Herrmann K, Scheurlen M, Buck AK, Kropf S, Wester HJ, Lapa C (2017) Imaging of chemokine receptor 4 expression in neuroendocrine tumors - a triple tracer comparative approach. Theranostics 7:1489–1498
12. Werner RA, Solnes LB, Javadi MS, Weich A, Gorin MA, Pienta KJ, Higuchi T, Buck AK, Pomper MG, Rowe SP, Lapa C (2018) SSTR-RADS version 1.0 as a reporting system for SSTR-PET imaging and selection of potential PRRT candidates: a proposed standardization framework. J Nucl Med 59:1085–1091
13. Rowe SP, Vicente E, Anizan N, Wang H, Leal JP, Lodge MA, Frey EC, Wahl RL (2015) Repeatability of radiotracer uptake in Normal abdominal organs with 111In-Pentetreotide quantitative SPECT/CT. J Nucl Med 56:985–988
14. Li X, Rowe SP, Leal JP, Gorin MA, Allaf ME, Ross AE, Pienta KJ, Lodge MA, Pomper MG (2017) Semiquantitative parameters in

PSMA-targeted PET imaging with ^{18}F-DCFPyL: variability in Normal-organ uptake. J Nucl Med 58:942–946
15. James WPT (1976) Research on obesity : a report of the DHSS/MRC group / compiled by W. P. T. James. London: HMSO:94
16. Mosteller RD (1987) Simplified calculation of body-surface area. N Engl J Med 317:1098
17. Garcia-Carbonero R, Garcia-Figueiras R, Carmona-Bayonas A et al (2015) Imaging approaches to assess the therapeutic response of gastroenteropancreatic neuroendocrine tumors (GEP-NETs): current perspectives and future trends of an exciting field in development. Cancer Metastasis Rev 34:823–842
18. Ayati N, Lee ST, Zakavi R, Pathmaraj K, al-Qatawna L, Poon A, Scott AM (2018) Long-acting somatostatin analog therapy differentially alters ^{68}Ga-DOTATATE uptake in Normal tissues compared with primary tumors and metastatic lesions. J Nucl Med 59:223–227
19. Boy C, Heusner TA, Poeppel TD, Redmann-Bischofs A, Unger N, Jentzen W, Brandau W, Mann K, Antoch G, Bockisch A, Petersenn S (2011) ^{68}Ga-DOTATOC PET/CT and somatostatin receptor (sst1-sst5) expression in normal human tissue: correlation of sst2 mRNA and SUVmax. Eur J Nucl Med Mol Imaging 38:1224–1236
20. Haug AR, Rominger A, Mustafa M, Auernhammer C, Goke B, Schmidt GP, Wangler B, Cumming P, Bartenstein P, Hacker M (2011) Treatment with octreotide does not reduce tumor uptake of ^{68}Ga-DOTATATE as measured by PET/CT in patients with neuroendocrine tumors. J Nucl Med 52:1679–1683
21. Soret M, Bacharach SL, Buvat I (2007) Partial-volume effect in PET tumor imaging. J Nucl Med 48:932–945